Supporting Online Material for

Lin28b reprograms adult bone marrow hematopoietic progenitors to mediate fetal-like lymphopoiesis

Joan Yuan[1], Cuong K. Nguyen[1], Xiuhuai Liu[1], Chrysi Kanellopoulou[1], Stefan A. Muljo[1*]

correspondence to: Stefan.Muljo@nih.gov

This PDF file includes:

Materials and Methods

Mice

WT and *Rag1*$^{-/-}$ mice on a C57BL/6 background were obtained from Taconic. *Il7ra*$^{-/-}$ and *Cd1d*$^{-/-}$ mice were obtained from Jackson Laboratory. All mice were maintained and treated in accordance with NIAID and Animal Care and Use Committee guidelines.

Antibodies

Antibodies were purchased as follows: anti-Lin28 rabbit polyclonal antibody (Cell Signaling Technology); anti-α-Tubulin clone DM1A (Sigma); anti-PLZF clone D-9 (Santa Cruz Biotechnology); anti-Vδ6.3/2-TCR clone 8F4H7B7 (BD Biosciences); Anti-NGFR clone ME20.4-1.H4 (Miltenyi Biotec); anti-CD5 clone 53-7.3, anti-B220 clone RA3-6B2, anti-CD1d clone 1B1, anti-CD23 clone B3B4, anti-CD19 clone 1D3, anti-γδ-TCR clone GL3, anti-CD3ε clone 17.A2, anti-CD4 clone GK1.5, anti-CD44 clone IM7, anti-NK1.1 clone PK136, anti-c-Kit clone 2B8, anti-HSA clone M1/69, anti-Sca-1 clone D7, anti-Gr-1 clone RB68C5, anti-CD93 clone AA4.1, anti-CD48 clone HM48-1, anti-CD150 clone 9D1, CD34 clone RAM34, anti-IgM clone II/41, anti-ESAM clone 1G8, anti-CD11b clone m1/70, anti-Eomes clone Dan11mag, Tie2 clone TEK4 (all from eBioscience). Anti-Vγ3 clone 536, anti-Vγ1 clone 2.11 and anti-Vγ2 clone UC3-10A6 were kindly provided by Drs. Karen Laky and B.J. Fowlkes (NIAID).

qRT-PCR

FACS-sorted cell populations were lysed for RNA extraction using RNAzol (Molecular Research Center, Inc) per manufacturer's instructions. For qRT-PCR, RNA was quantitated using a NanoDrop spectrophotometer (Thermo Fisher Scientific) and reverse transcribed using the TaqMan reverse transcription kit (Applied Biosystems). Real-time PCR was performed using the KAPA probe fast 2x master mix (KAPA biosystems) in a

7900HT Fast Real-Time PCR instrument (Applied Biosystems). TaqMan assays for *mLin28b*, *mGAPDH*, *hLin28b*, *hHPRT* and TaqMan miRNA assays for U6 and let-7 family members were obtained from Applied Biosystems. The TaqMan miRNA assays utilize stem-loop primers for specific reverse transcription of the mature miRNAs. Primetime qPCR probes for *Tal1*, *Mecom*, *Igf2* and *Hmga2* were obtained from Integrated DNA Technologies. C_T values from triplicate samples were averaged and relative expression was calculated using the $2\text{-}\Delta\Delta C_T$ method. Human fetal total RNA samples were obtained from Clontech and pooled from at least six spontaneously aborted fetuses (22-40 weeks of gestation). Human adult total RNA samples were obtained as a part of the FirstChoice® Total RNA: Human Normal Tissue panel from Ambion and were pooled from at least 3 tissue donors. Total cDNA from human $CD34^+$ cord blood cells were pooled from four donors and was obtained from DVBiologics. Commercially purchased human RNA and cDNA samples were under full informed consent and IRB approvals obtained by the distributors.

miRNA profiling and RNA-seq

For miRNA profiling and RNA-seq analysis, total RNA was extracted from FACS-sorted populations from at least 3 recipient mice or 12 fetal livers as described above. RNA concentration was determined using the Qubit RNA broad range assay in the Qubit Fluorometer (Invitrogen). To confirm the concentration and determine the integrity of the RNA we used the Eukaryote Total RNA Nano Series II chip on a 2100 Bioanalyzer (Agilent). 100 ng of total RNA was used as the starting material for miRNA profiling using the nCounter Mouse miRNA Expression Assay platform (NanoString Technologies). Sample preparation and flow-cell hybridization was performed per manufacturer's instructions at the DNA Sequencing and Digital Expression Core Facility (National Cancer Institute). Per manufacturer's instructions, data were normalized to the sum of positive control count values provided in assay to account for lane to lane variation. Background determination was set by the mean + 2x standard deviation of 8 negative control detectors. For pro-B cells, expression counts were normalized to the

sum of the counts of the 75 highest expressing miRNAs in each sample. let-7 miRNAs that fell into the category of the 75 highest expressing miRNAs were excluded from the list. For DP thymocytes, expression counts were normalized to the mean signal level of a number of house-keeping genes (*Actb, B2m, Gapdh, Rpl19, Rplp0*). RNA-seq library preparation was performed starting with 3.3 μg of total RNA using the TruSeq RNA sample prep kit following manufacturer's protocol (Illumina). Briefly, oligo-dT purified mRNA was fragmented and subjected to first and second strand cDNA synthesis. cDNA fragments were blunt-ended, ligated to Illumina adaptors, and PCR amplified to enrich for the fragments ligated to adaptors. The resulting cDNA libraries were verified and quantified on Agilent Bioanalyzer, and paired-end RNA-seq was conducted using the GAIIx Genome Analyzer (Illumina).

RNA-Seq and miRNA signature analyses

RNA-Seq paired-end reads were aligned to the mouse genome (NCBI 37, mm9) using the spliced read aligner TopHat version 1.3.1 with option --mate-inner-dist 160 --coverage-search --microexon-search --max-multihits 20 (*53*). Briefly, using a two step mapping processes, TopHat first uses Bowtie version 0.12.7 (*54*) to align reads that are directly mapped to the genome (with no gaps). It then determines the possible location of gaps in the alignment based on canonical and non-canonical splice sites flanking the aligned reads. Finally, it uses gapped alignments to align the reads that were not aligned by Bowtie in the first step. Aligned reads were visualized on a local mirror of the UCSC Genome Browser (*55*).

Gene expression quantification was performed by counting aligned reads on each transcript for each condition using in-house codes. A ranked gene list from up-regulated to down-regulated based on the $\log_2$ of a ratio of the expressions of each gene in the two conditions was then supplied to Sylamer version 08-123 (*56*) to statistically calculate the enrichment of seed sequences of all known miRNAs (version 15 from miRbase.org). A list of 175 putative target genes were identified by choosing up-regulated genes

containing the statistically enriched let-7 binding site motif (TACCTCA) that pass the E-value threshold (Bonferroni-corrected) of *P*-value < 0.01. This list was then compared against the 446 and 683 putative let-7 miRNA family target mRNAs computationally predicted by PicTar (http://pictar.mdc-berlin.de/) and TargetScan (http://www.targetscan.org/) respectively (*20, 21*). The False Discovery Rate (FDR) of the overlapped genes was then estimated by shuffling the RefSeq gene list 1000 times, randomly picking up 446 and 683 genes and getting the average number of genes that overlap with the Sylamer let-7 target gene list, which are 4.5 and 6.9 respectively. The FDR for the overlapped genes (4.5 out of 47 and 6.9 out of 67 genes) then is about 10% for both comparisons.

Retrogenic BM chimeras

Mouse *Lin28* and human *Lin28b* cDNA were PCR amplified from cDNA clones obtained from Origene and subcloned into a MSCV-IRES-GFP based vector, a kind gift of Ken Murphy (*19*). Plasmid inserts were verified by sequencing. Viral supernatants were generated as previously described (*57*). Mouse *Lin28* cDNA was later cloned into a MSCV-IRES-hNGFR vector (kind gift of Tim Bender, Univ. of Virginia) as seen in Fig. S11B. BM cells were collected from the femurs and tibiae of 6-8 week old donor mice and FL cells were collected from embryos 13.5-14.5 dpc. After red blood cell lysis, HSPCs were enriched by autoMACS depletion of lineage positive cells using the Lineage Cell Depletion Kit (Miltenyi) for BM cells and biotinylated antibodies to Gr-1, B220 and Ter119 (eBiosciences) and anti-biotin beads (Miltenyi) for FL cells. Negatively selected cells were cultured in chemically defined serum free medium X-vivo 10 with Gentamicin (Lonza) supplemented with L-glutamine (1x) (Gibco), beta-mercaptoethanol (50mM), mouse recombinant SCF (50 ng/ml), IL-6 (10 ng/ml), IL-3 (5ng/ml), FLT-3L (5ng/ml) and IL- 7 (5ng/ml) (Peprotech). The following day, co-cultures were transduced by spin-infection at 700 × g at 32 ^{o}C for 90 minutes in the presence of retroviral supernatant and 5 µg/ml polybrene (Sigma-Aldrich). Cells were incubated for another 4 hours prior to tail vein injection into recipient mice at 2-4 million cells per mouse in 200 ml sterile PBS.

Recipient mice were 6 weeks or older and irradiated at 450 RADs at least 4 hours prior to adoptive transfer. Recipient mice were analyzed by flow cytometry 6-8 weeks following adoptive transfer unless otherwise noted.

Flow cytometry and cell sorting

Single cell suspension was stained as described (*58*). Samples were collected on an LSR II (BD) or sorted on a FACS Aria II (BD) and data were analyzed with FlowJo software (TreeStar). Intracellular stainings of PLZF and Eomes were performed using the Foxp3 staining buffer set (eBiosciences) per manufacturer's instructions. iNKT cells were identified with APC or PE-conjugated mouse CD1d tetramer loaded with PBS57 ($CD1d^{PBS57}$) provided by the NIH Tetramer Core Facility at Emory University. For *in vitro* cell cycle analysis, BM HSPCs were transduced as described above and cultured for an additional 48 hours prior being pulsed for 1 hour with 10 μM EdU. Pulse labeled cells were then stained using the Click-iT® EdU Flow Cytometry Assay Kit (Invitrogen) per manufacturer's instructions.

Supplementary Figures

Name	Chr.	Sequence
miR-98	X (intronic)	ugagguaguaaguuguauuguu
let-7f-2	X (intronic)	ugagguaguagauuguauaguu
let-7a-1	13 (intergenic)	ugagguaguagguuguauaguu
let-7f-1	13 (intergenic)	ugagguaguagauuguauaguu
let-7d	13 (intergenic)	agagguaguagguugcauaguu
Let-7e	17 (intergenic[1])	ugagguaggagguuguauaguu
let-7c-2	15 (intergenic)	ugagguaguagguuguaugguu
let-7b	15 (intergenic)	ugagguaguagguugugugguu
let-7c-1	16 (intronic[2])	ugagguaguagguuguaugguu
let-7a-2	9 (intergenic[3])	ugagguaguagguuguauaguu
let-7g	9 (intronic)	ugagguaguaguuuguacaguu
let-7i	10 (intergenic)	ugagguaguaguuugugcuguu

[1]clustered with mir-99b and mir-125a
[2]clustered with mir-99a
[3]clustered with mir-100

Fig. S1. An alignment of the mature miRNA sequences of the twelve let-7 isomiRs encoded in the mouse genome is shown along with chromosomal location (Chr.). Sequences were obtained from miRBase (http://www.mirbase.org/) (*59*). Conserved seed sequences are shown in red.

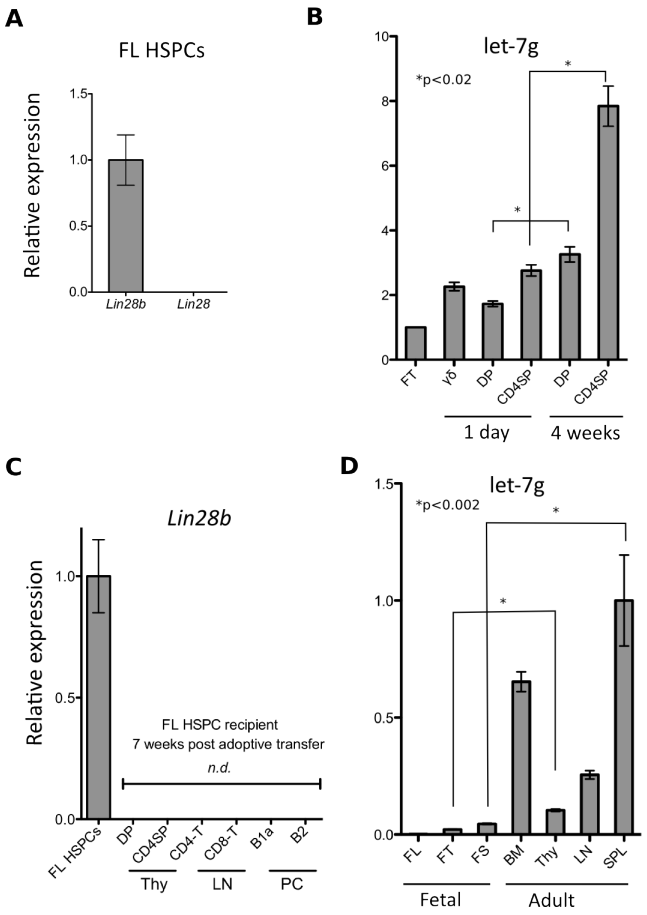

Fig. S2. *Lin28b* and let-7g are differentially expressed during fetal and adult hematopoiesis. **(A)** Graph shows relative abundance (arbitrary units) of mouse *Lin28* and *Lin28b* measured by qRT-PCR in FACS-sorted Lin^{-ve} FL HSPCs. **(B)** qRT-PCR of mature let-7g expression using TaqMan assay in FACS-sorted thymocyte populations from wild-type C57BL/6 mice of the indicated age. **(C)** qRT-PCR of *Lin28b* of the indicated populations from FACS sorted populations pooled from two sub-lethally irradiated *Rag1*$^{-/-}$ recipients of FL HSPCs. Thymus (Thy) DP ($CD4^{+}CD8^{+}CD3^{lo}$), CD4SP ($CD4^{+}CD8^{-ve}CD3^{+}$). Lymph node (LN) CD4-T ($CD3^{+}CD4^{+}$), CD8-T ($CD3^{+}CD8^{+}$). Peritoneal cavity (PC) B-2 ($CD19^{+}$ $B220^{hi}$ $CD5^{-ve}$), B-1a ($CD19^{+}$ $B220^{lo}$ $CD5^{+}$). **(D)** qRT-PCR of mature let-7g expression in the indicated fetal and adult human organs. * indicates statistical significance calculated by *t*-test. *n.d.* indicates not detectable.

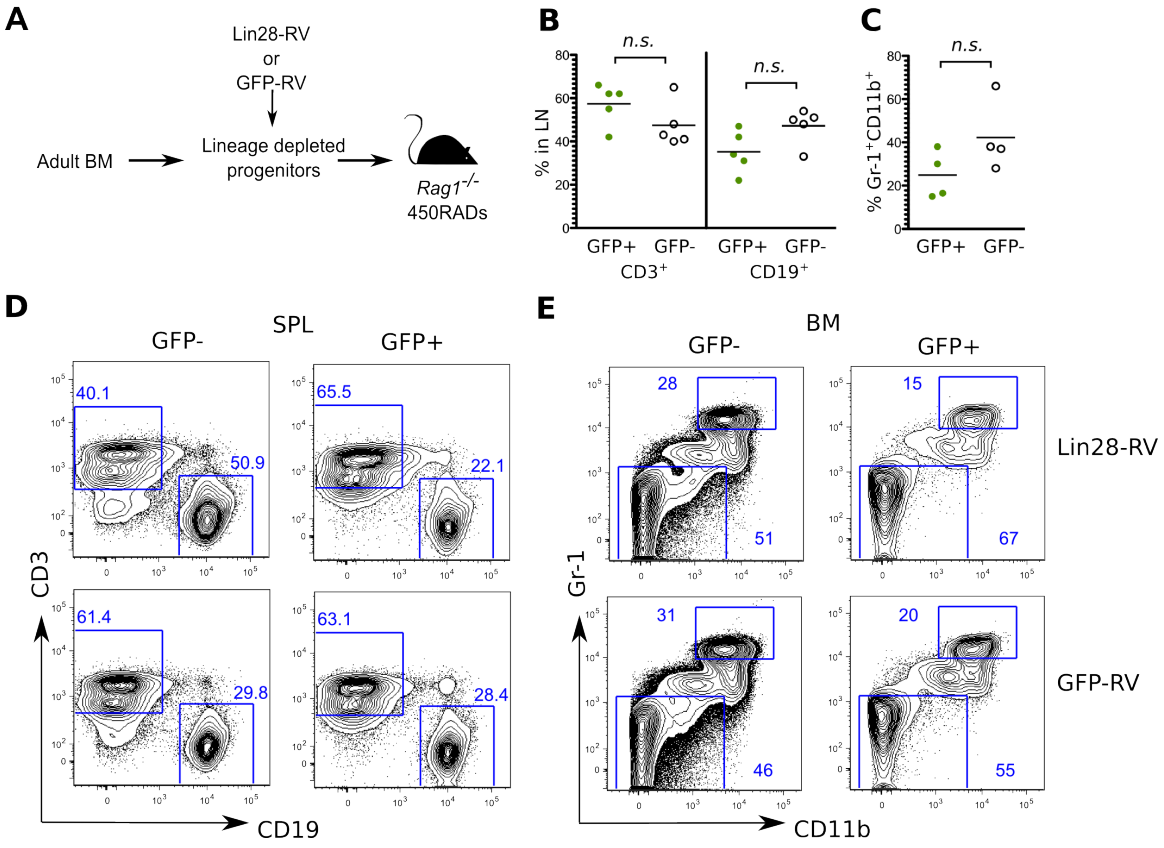

Fig. S3. (A) Scheme for retrogenic BM chimera is shown. HSPCs of adult BM origin were transduced with Lin28-encoding (Lin28-RV) or control (GFP-RV) retrovirus and injected into sub-lethally irradiated *Rag1*$^{-/-}$ recipients. **(B)** The percent of CD3^{+} T cells and CD19^{+} B cells within the GFP^{+} and GFP^{-ve} lymph node (LN) populations from five independent Lin28-RV BM chimeras are shown. **(C)** The percent of Gr-1^{+}CD11b^{+} myeloid cells among GFP^{+} and GFP^{-ve} BM cells from four independent Lin28-RV BM chimeras are shown. Statistical significance was calculated by *t*-test. *n.s.* indicates not statistically significant. **(D)** FACS analysis shows an example of the distribution of CD3^{+} versus CD19^{+} populations within the GFP^{+} and GFP^{-ve} lymph node subsets in Lin28-RV and GFP-RV chimeras.

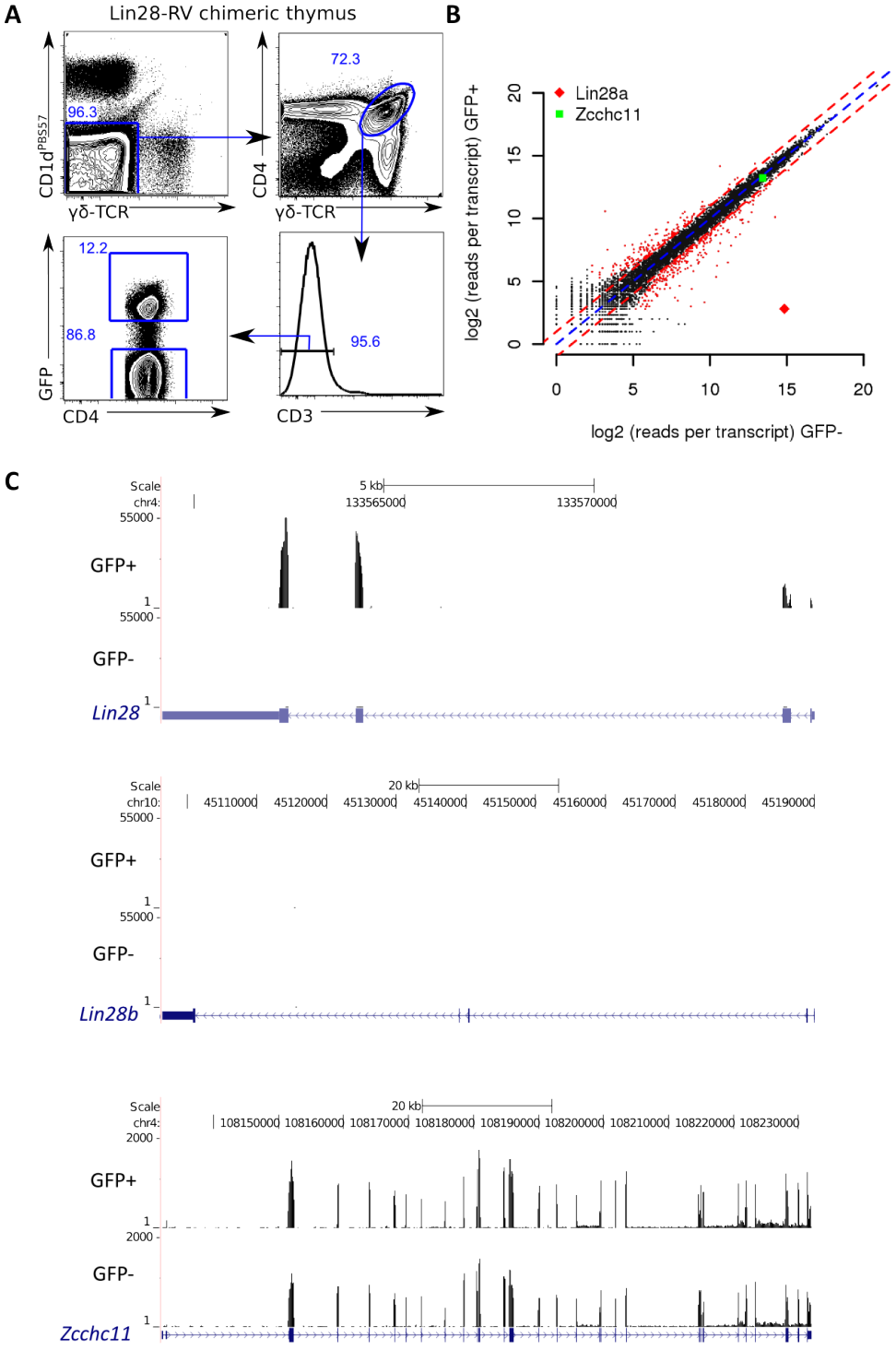

Fig. S4. (A) FACS plots illustrate sorting scheme of pre-selection DP thymocytes for miRNA profiling and RNA-seq. GFP^{+} and GFP^{-ve} DP thymocytes were sorted through a

$CD1d^{PBS57\text{-}ve}$ γδ-TCR^{-ve} $CD3^{-ve}$ gate. **(B)** Results of paired-end RNA-seq of FACS-sorted GFP^{+} and GFP^{-ve} DP ($CD4^{+}CD8^{+}CD3^{lo}$) thymocytes pooled from three Lin28-RV BM recipients are depicted. Scatter plot of expression levels (log_2 of number of reads for each gene) of all 20,096 transcripts in GFP^{-ve} versus GFP^{+} DP thymocytes. *Lin28* expression is marked by a red diamond. *Zcchc11*, encoding TUT4, a terminal uridyl transferase required for *Lin28/Lin28b* mediated poly-uridylation and degradation of pre-let-7 (*14*), is marked by a green square. **(C)** Screenshots of RNA-seq coverage tracks are shown for the indicated transcripts. *Top*: ectopic Lin28 expression accounts for the highest differentially expressed mRNA between the 2 groups. The retroviral Lin28 cDNA insert does not contain the 3' UTR; as a result, no expression is detected for the 3' UTR. *Middle*: Endogenous *Lin28b* is not detectable. *Bottom*: *Zcchc11* mRNA is equally expressed in the populations compared.

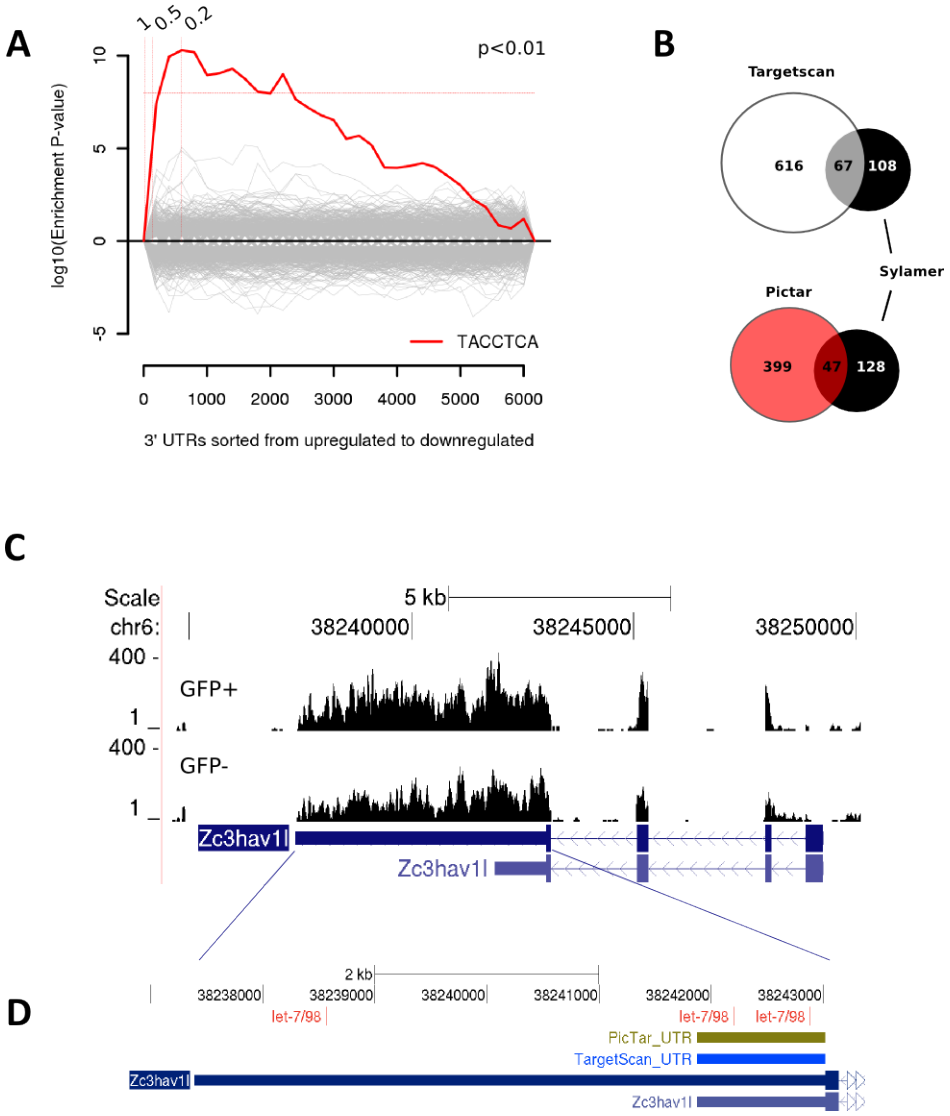

Fig. S5. (A) Sylamer analysis (*56*) of RNA-seq data depicted in a landscape plot demonstrates enrichment of the complementary let-7 family heptameric seed sequence TACCTCA (red line) in 3' UTRs among up-regulated genes. The x-axis represents the sorted gene list from most up- regulated (left) to most down-regulated (right). The y-axis shows the hypergeometric significance for enrichment of heptamers in 3' UTRs among genes. The horizontal dotted lines represent an E-value threshold (p-value Bonferroni-corrected for multiple testing) of 0.01. Vertical dotted lines indicate $\log_2$ fold change cutoffs of >1.0, >0.5 and >0.2. **(B)** Venn diagrams illustrate the comparisons between putative target genes identified by Sylamer analysis of RNA-Seq data and two widely-used computational prediction methods, PicTar (*21*) and TargetScan (*20*). 67 out of 175

target mRNAs from the Sylamer analysis overlap with 683 evolutionarily conserved let-7 targets predicted by TargetScan. 47 out of 175 target mRNAs from the Sylamer analysis overlap with 446 evolutionarily conserved let-7 targets predicted by PicTar. In contrast, when random genes were selected instead of the TargetScan or PicTar predicted targets, there was a false discovery rate (FDR) of 10% for both comparisons (see Material and Methods). **(C)** RNA-Seq coverage track of *Zc3hav1l* – the top putative target identified in (B), is predicted to have a short and a long 3' UTR. Screenshots of RNA-seq coverage tracks are shown to indicate that in DP thymocytes, the isoform with the long 3' UTR is expressed. Consequently, there is a third putative let-7 binding site that is not predicted by TargetScan or PicTar because they only considered the short 3' UTR. *Top*, coverage for GFP^{+} RNA-seq; *bottom*, coverage for GFP^{-ve} RNA-seq visualized using UCSC genome browser (*55*)**. (D)** Magnified view of the 3' UTR region of Zc3hav1l indicates three let-7 family seed motifs and 3' UTR coordinates used by TargetScan and PicTar.

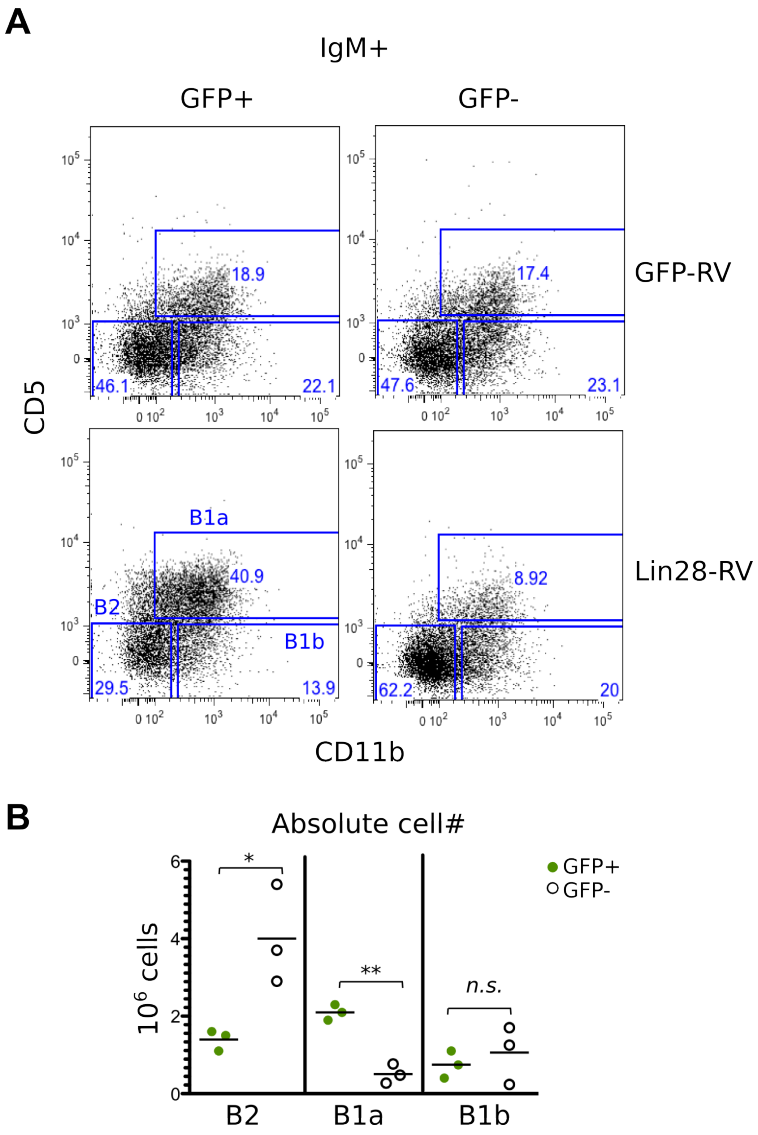

Fig. S6. (A) FACS analysis show alternative flow cytometric analyses of peritoneal cavity (PerC) B-cell subsets in Lin28-RV and GFP-RV BM chimeras according to Barber *et al*, 2011 (*11*). Data are representative of 4 separate reconstitution experiments. **(B)** Graph shows the average absolute numbers of of B-2 ($IgM^{+}CD11b^{-ve}CD5^{-ve}$), B-1a ($IgM^{+}CD11b^{+}CD5^{+}$) and B-1b ($IgM^{+}CD11b^{+}CD5^{-ve}$) B-lymphocytes among the GFP^{+} and GFP^{-ve} fractions of peritoneal cavity cells in four independent Lin28-RV BM chimeras. * $P<0.05$ ** $P<0.01$ indicate statistical significance calculated by *t*-test. *n.s.* indicates not statistically significant.

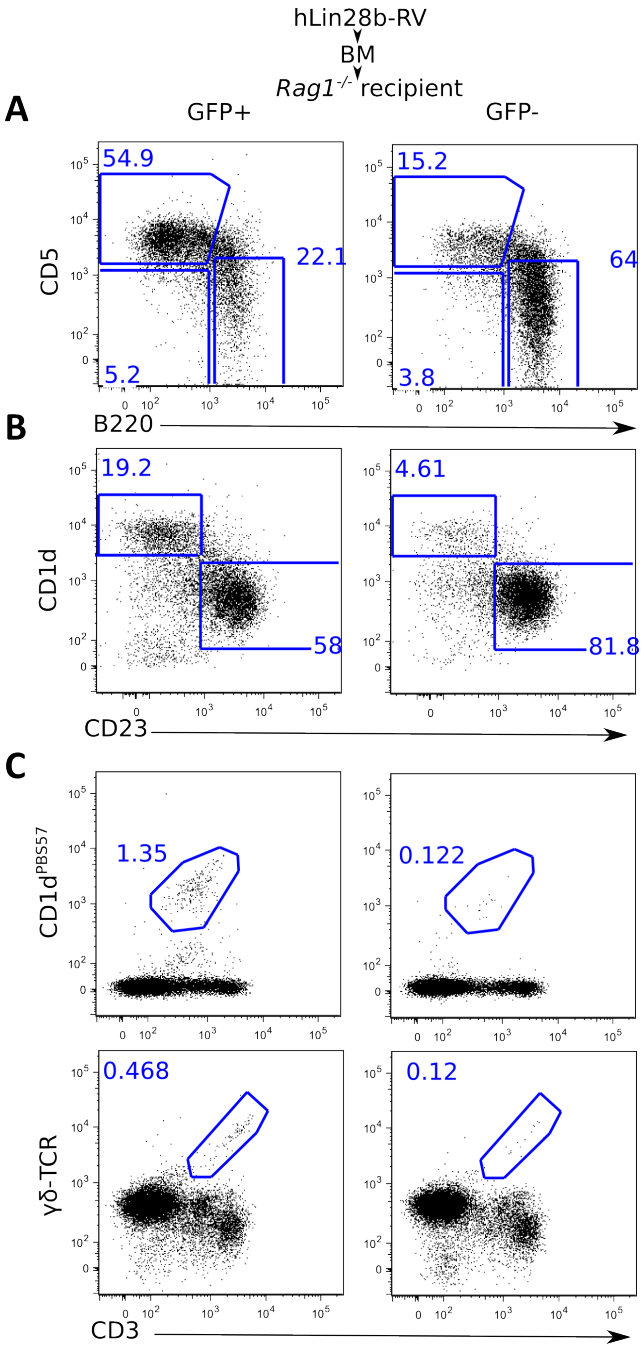

Fig. S7. Ectopic hLin28b expression in adult BM HSPCs phenocopies ectopic mLin28 expression. FACS analysis of the GFP^{+} and GFP^{-ve} lymphocyte fractions in hLin28b-RV BM chimeras: **(A)** CD19^{+} peritoneal cavity B-cell subsets, **(B)** splenic B cell subsets and **(C)** total thymocytes.

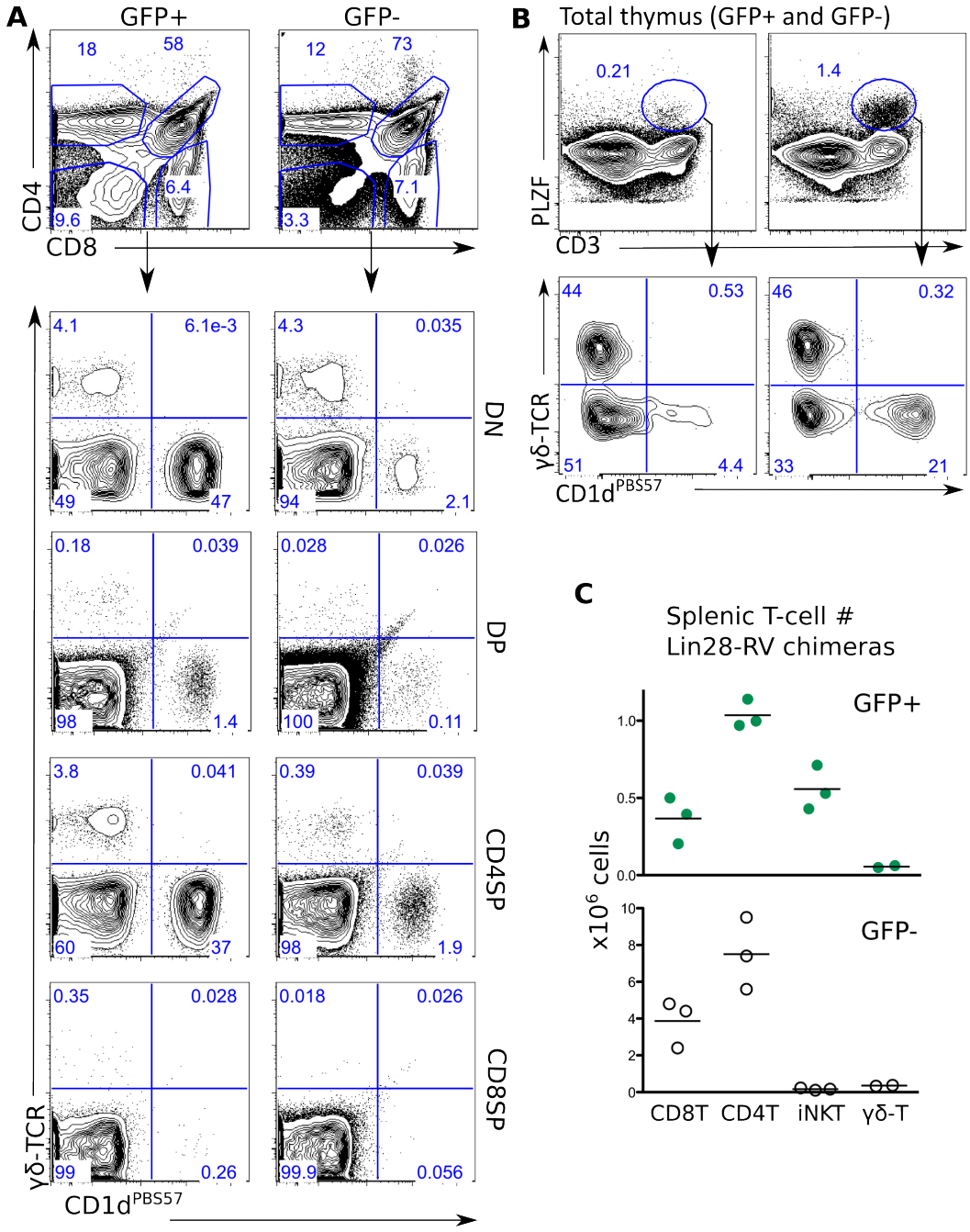

Fig. S8. (A) *Upper panel:* Flow cytometric analysis of the Lin28-RV recipient thymus. Plots show CD4 versus CD8 profiles among GFP^{+} and GFP^{-ve} thymocytes in Lin28-RV BM recipients 6 weeks post-adoptive transfer. *Lower panel:* Plots show flow cytometry of gd-TCR^{+} and CD1d^{PBS57+} iNKT cells in the indicated thymocyte compartments. **(B)**

Intracellular staining of PLZF in thymocytes of Lin28-RV and GFP-RV BM chimeras. Total thymocytes were analyzed since intracellular staining method used did not allow for detection of GFP. **(C)** Graphs show absolute cell numbers of the indicated T cell populations in the GFP^{+} (green) and GFP^{-ve} (white) fractions of the Lin28-RV BM recipient spleen.

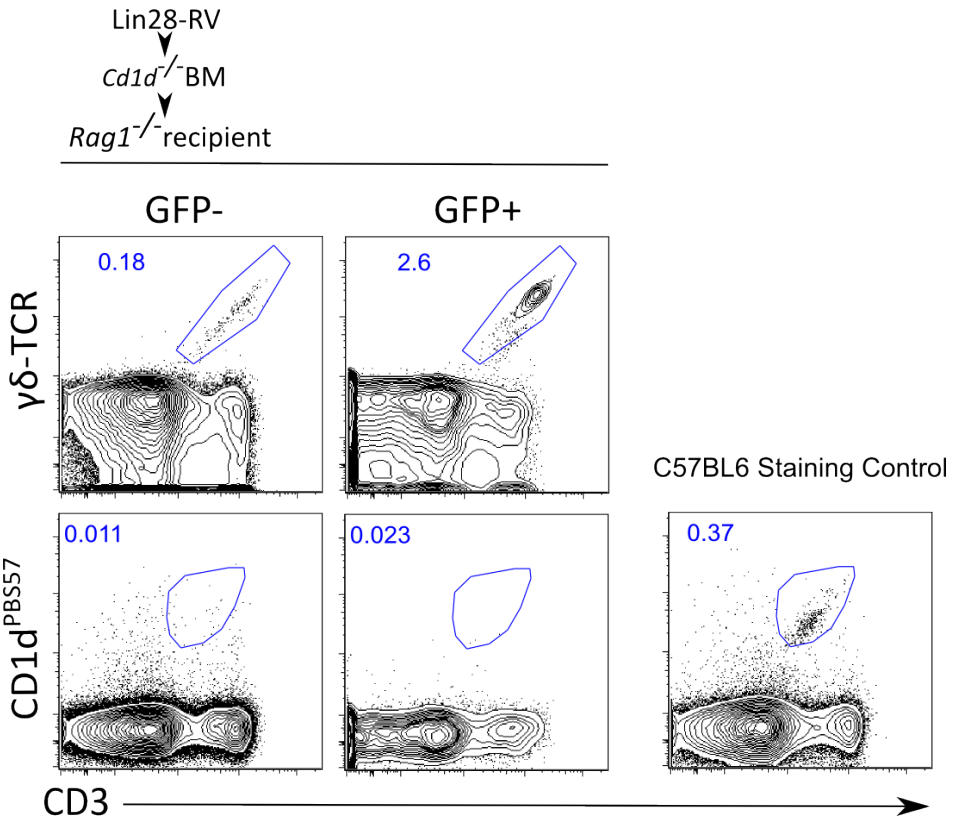

Fig. S9. Lin28-induced iNKT cells are CD1d dependent. Flow cytometric analysis of BM chimeras reconstituted with Lin28-RV transduced *Cd1d*$^{-/-}$ BM HSPCs. Recipient thymocytes were assessed for the presence of γδ-T and iNKT cells. Thymocytes from an intact C57BL/6 mouse was used as a $CD1d^{PBS57}$ staining control (far right).

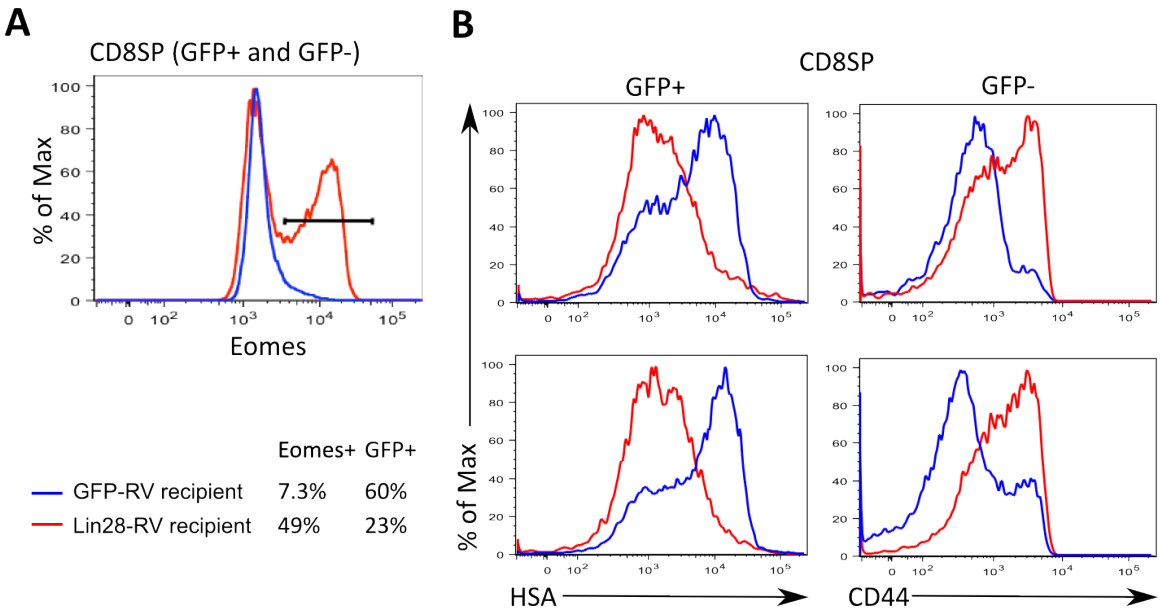

Fig. S10. (A) Intracellular staining of Eomes in total CD8SP thymocytes in the Lin28-RV (red line) and GFP-RV BM (blue line) recipient. Intracellular staining method used did not allow for detection of GFP. Percentage GFP^+ cells in the CD8SP population was determined separately as indicated. The percentage of GFP^+ CD8SP thymocytes cannot account for the increase in $Eomes^+$ CD8SP thymocytes consistent with the well-characterized bystander effect (*34*). **(B)** Surface expression of CD44 and HSA show memory-like phenotype ($CD44^{hi}HSA^{-ve}$) in both GFP^+ and GFP^{-ve} CD8SP thymocytes of Lin28-RV compared to GFP-RV BM recipients.

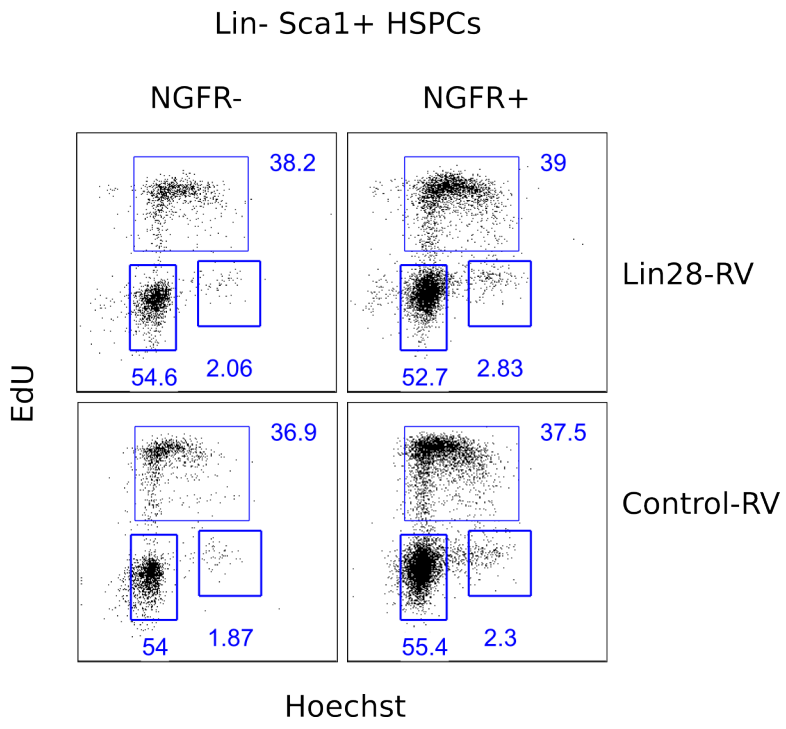

Fig. S11. Cell cycle analysis of Lin28-RV transduced bone marrow HSPCs *in vitro*. Wild type C57BL/6 bone marrow HSPCs were transduced with the indicated viruses and pulsed with EdU for 1 hour at 48 hours post transduction. FACS plots show EdU-uptake and DNA content analysis of transduced and untransduced HSPCs (Lin^{-ve} $Sca\text{-}1^{+}$) in culture.

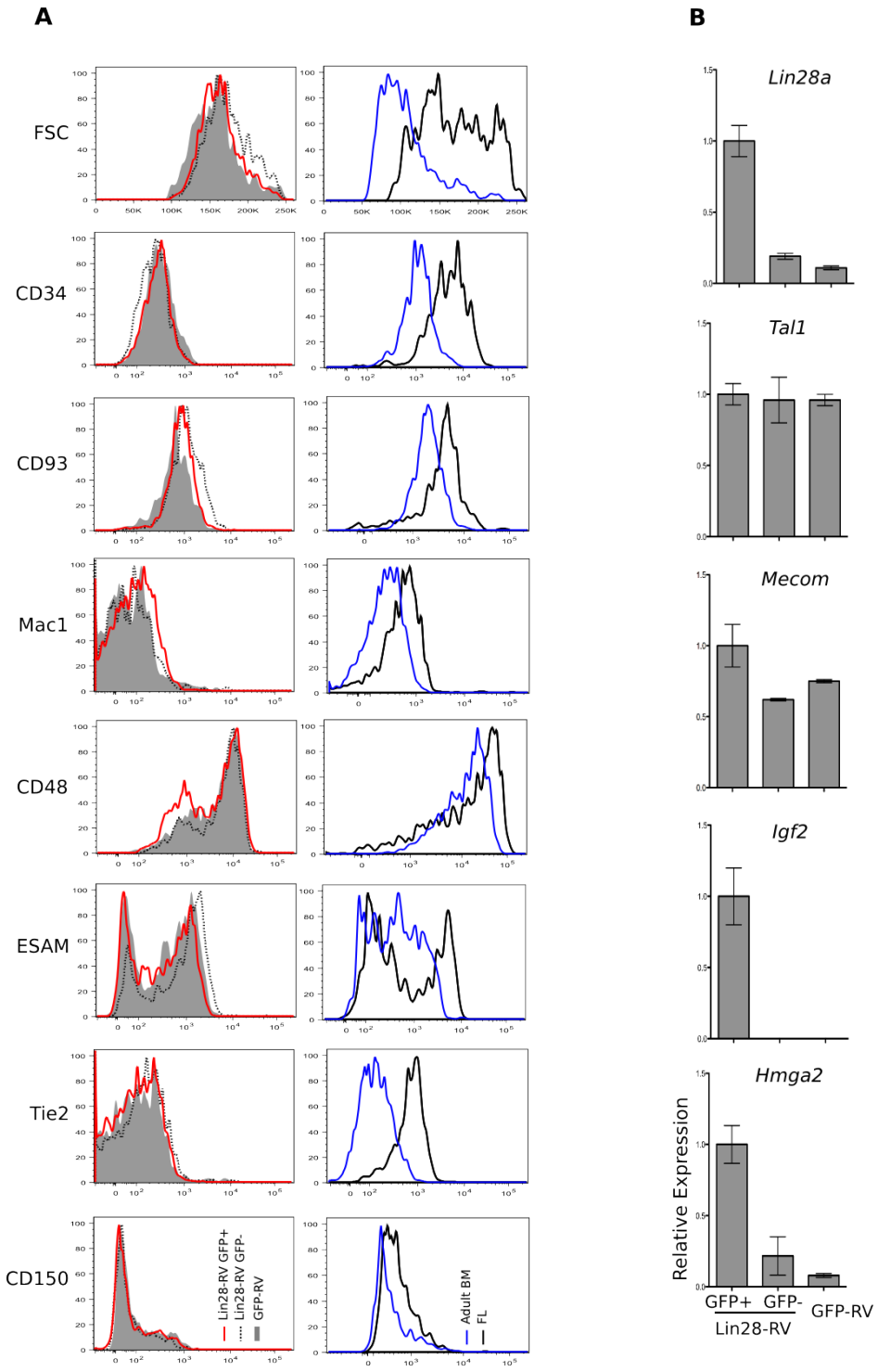

Fig. S12. (A) FACS analysis of the indicated surface markers in freshly isolated BM LSK HSCs from (left) Lin28-RV and GFP-RV BM chimeras; (right) FL and adult BM. **(B)** qRT-PCR analysis of the indicated transcripts in FACS sorted LSK HSC populations

from Lin28-RV and GFP-RV BM chimeras. Due to the extreme rarity in the occurrence of LSK HSC cells, the GFP^{+} and GFP^{-ve} populations in the control GFP-RV chimeras were not separately analyzed.

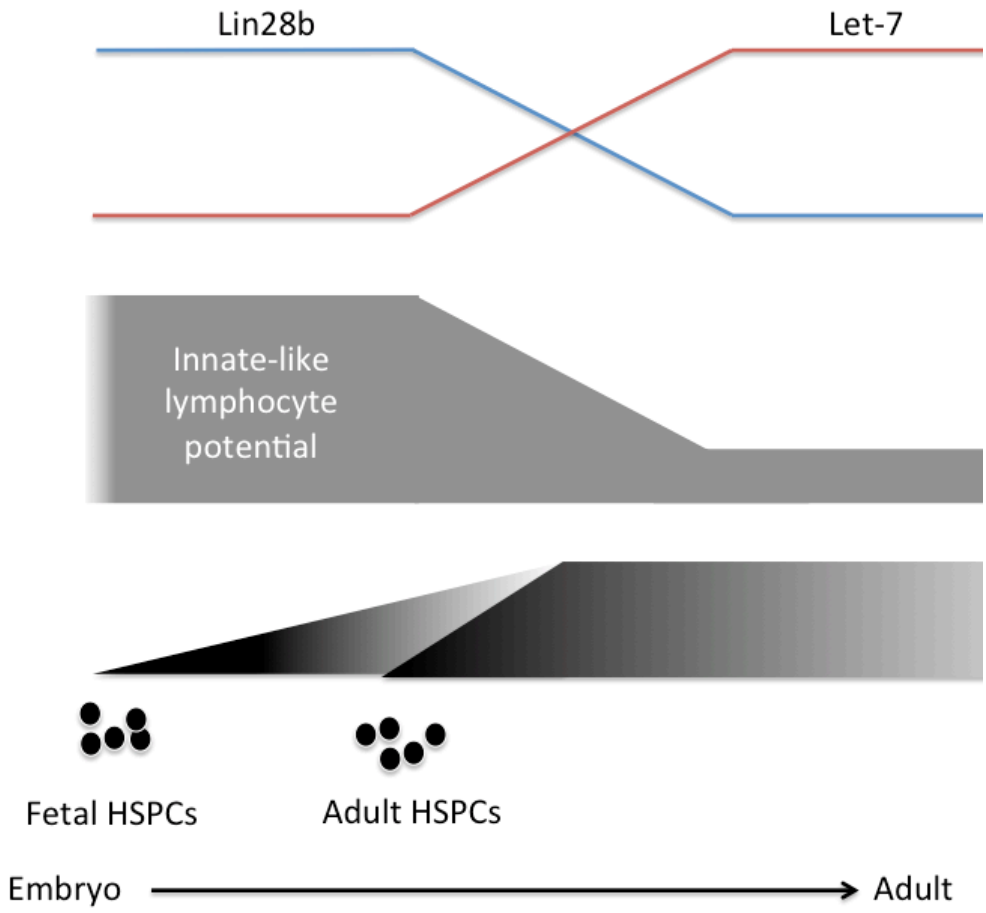

Fig. S13. Model depicting how the Lin28b/Let-7 axis correlates with fetal and adult hematopoiesis. *Lin28b* is highly expressed in fetal HSPCs (eg. fetal liver and thymus) in humans and mice but is down-regulated in the neonate and undetectable in adult HSPCs. The expression of *Lin28b* is inversely correlated to expression of mature let-7 family members, but it is correlated with the potential of fetal HSPCs to mediate development of innate-like lymphocytes (eg. B-1a, MZ B, iNKT and certain γδ-T cells).

Supplementary Tables

Table S1.

List of 47 genes overlapping between 175 putative target genes containing complementary let-7 family seed motif (TACCTCA) identified using Sylamer and 446 putative let-7 miRNA family target mRNAs computationally predicted by PicTar (*21*). Genes also predicted by TargetScan are highlighted in yellow.

RefSeq	Gene Symbol	UTR size	$\log_2$ Fold Change	TACCTCA motif in UTR
NM_172467	Zc3hav1l	5626	0.46	3
NM_130447	Dusp16	2411	0.43	1
NM_001029890	Mex3a	4195	0.41	1
NM_029850	Bcl7a	2993	0.40	1
NM_001033275	Gxylt1	5412	0.38	2
NM_177242	Pptc7	3407	0.38	1
NM_178389	Gale	315	0.37	1
NM_008377	Lrig1	1223	0.35	1
NM_172839	Ccnj	1911	0.35	1
NM_026075	Srek1ip1	1726	0.35	1
NM_016706	Coil	869	0.34	1
NM_011945	Map3k1	740	0.34	1
NM_025872	Golt1b	2277	0.32	1
NM_007520	Bach1	3475	0.32	2
NM_175212	Tmem65	2640	0.28	1
NM_133750	Fam118a	1277	0.27	1
NM_026856	Zfp644	1494	0.24	1
NM_198421	Usp49	5866	0.23	1

NM_013814	Galnt1	776	0.22	2
NM_175472	Zcchc11	630	0.22	1
NM_023336	Brd3	2886	0.22	1
NM_133803	Dpp3	393	0.21	1
NM_016898	Cd164	2200	0.20	1
NM_026635	Fam96a	521	0.20	1
NM_178922	Hic2	4261	0.20	2
NM_029999	Lbh	2498	0.19	1
NM_001004164	Gnptab	1489	0.19	1
NM_144551	Trib2	1881	0.19	1
NM_031494	Zfp275	4697	0.18	1
NM_133794	Qars	95	0.18	1
NM_011947	Map3k3	1238	0.17	1
NM_028876	Tmed5	2914	0.16	1
NM_207636	Fndc3a	2216	0.16	1
NM_010937	Nras	3727	0.15	1
NM_009211	Smarcc1	2265	0.14	1
NM_177475	Zfp280b	3236	0.14	1
NM_173753	Fnip1	2659	0.13	1
NM_018771	Gipc1	412	0.13	1
NM_178668	Pde12	504	0.13	1
NM_177103	Senp5	921	0.13	1
NM_013760	Dnajb9	1057	0.12	1
NM_008465	Kpna1	3223	0.12	1
NM_199322	Dot1l	1947	0.12	1
NM_026367	Gpatch2	2850	0.11	1
NM_013860	Limd1	2274	0.11	1
NM_172683	Pogz	1994	0.11	1

NM_013586	Loxl3	1686	0.11	1

Table S2.

List of 67 genes overlapping between 175 putative target genes containing complementary let-7 family seed motif (TACCTCA) identified using Sylamer and 683 putative let-7 miRNA family target mRNAs computationally predicted by TargetScan (*20*). Genes also predicted by PicTar are highlighted in yellow.

RefSeq	**Gene Symbol**	**UTR size**	**log_2 fold change**	**TACCTCA motif in UTR**
NM_172467	Zc3hav1l	5626	0.46	3
NM_130447	Dusp16	2411	0.43	1
NM_001142655	Arpp19	3508	0.42	1
NM_001039644	Edem3	3338	0.41	1
NM_001029890	Mex3a	4195	0.41	1
NM_029850	Bcl7a	2993	0.40	1
NM_001146025	Rnf44	2348	0.39	1
NM_177242	Pptc7	3407	0.38	1
NM_178389	Gale	315	0.37	1
NM_008771	P2rx1	1071	0.37	1
NM_176958	Hif1an	5116	0.36	4
NM_008377	Lrig1	1223	0.35	1
NM_172839	Ccnj	1911	0.35	1
NM_019683	Ankrd49	941	0.34	1
NM_016706	Coil	869	0.34	1
NM_011945	Map3k1	740	0.34	1
NM_025872	Golt1b	2277	0.32	1
NM_007520	Bach1	3475	0.32	2
NM_029736	Slc10a7	2365	0.29	2
NM_009191	Clpb	2415	0.29	1

NM_175212	Tmem65	2640	0.28	1
NM_001081221	Ercc6	3887	0.28	1
NM_001033422	Thoc2	2807	0.27	1
NM_053103	Entpd7	3762	0.25	1
NM_026856	Zfp644	1494	0.24	1
NM_001081229	Tsc22d2	6519	0.24	1
NM_009906	Tpp1	1614	0.24	1
NM_025994	Efhd2	1605	0.24	1
NM_198421	Usp49	5866	0.23	1
NM_001127363	Inpp5a	1306	0.23	1
NM_175313	A130022J15Rik	2036	0.23	1
NM_026376	Plxnd1	929	0.22	1
NM_026869	Pygo2	1614	0.22	1
NM_013814	Galnt1	776	0.22	2
NM_023336	Brd3	2886	0.22	1
NM_134133	2010002N04Rik	1203	0.21	1
NM_133803	Dpp3	393	0.21	1
NM_172015	Iars	518	0.21	1
NM_010751	Mxd1	1889	0.20	1
NM_178922	Hic2	4261	0.20	2
NM_029999	Lbh	2498	0.19	1
NM_001004164	Gnptab	1489	0.19	1
NM_144551	Trib2	1881	0.19	1
NM_031494	Zfp275	4697	0.18	1
NM_133794	Qars	95	0.18	1
NM_001080746	Gtf2i	1072	0.17	1
NM_011947	Map3k3	1238	0.17	1
NM_001008550	Zfyve26	1619	0.17	1

NM_028876	Tmed5	2914	0.16	1
NM_001081048	Slc25a18	693	0.16	1
NM_172876	Gpatch3	411	0.16	1
NM_207636	Fndc3a	2216	0.16	1
NM_010937	Nras	3727	0.15	1
NM_010813	Mnt	2405	0.14	1
NM_011062	Pdpk1	5346	0.14	1
NM_001040400	Tet2	2898	0.14	1
NM_145384	Pqlc2	1446	0.14	1
NM_009211	Smarcc1	2265	0.14	1
NM_177475	Zfp280b	3236	0.14	1
NM_173753	Fnip1	2659	0.13	1
NM_018771	Gipc1	412	0.13	1
NM_177103	Senp5	921	0.13	1
NM_013760	Dnajb9	1057	0.12	1
NM_144873	Uhrf2	858	0.12	1
NM_199322	Dot1l	1947	0.12	1
NM_026367	Gpatch2	2850	0.11	1
NM_013860	Limd1	2274	0.11	1